TRA suggests that the conditions that favor parasitism of other species are unlikely to be simple elaborations of the conditions selecting for parasitism of conspecifics.

One line of evidence used to promote this hypothesis has been refuted by the cowbird phylogeny presented herein. Payne (*2*) suggested that INTRA followed by the development of INTER explained the parasite-host relationship between *M. rufoaxillaris* and *M. badius*. However, Payne assumed that these two species were closely related. This assumption now appears invalid.

The apparent distance between *M. rufoaxillaris* and *M. badius* is of added interest in light of their plumage morphologies. Although adult plumages are distinctive (*M. rufoaxillaris* is predominantly black and *M. badius* is predominantly light gray) the nestling plumages are nearly indistinguishable (*1, 16, 17*). Hudson (*16*) and Friedmann (*1*) concluded that this similarity reflected recency of common descent rather than any form of mimicry on the part of the parasite. They supported this argument with the observation that other brood parasites are quite successful at parasitizing hosts morphologically dissimilar from themselves without employing any form of nestling mimicry. However, the results presented herein refute the hypothesis that these two taxa are sister taxa. Even if *M. badius* is the sister taxon to the remaining cowbirds (the current data are uninformative about this question), these results suggest that these two taxa have not shared a common ancestor for a considerable period of time. Therefore, the similarity in nestling plumage patterns, whether due to convergence or parallelism, suggests that there is an advantage derived by *M. rufoaxillaris* as a result of the close resemblance of its young to those of the host species.

The lack of data uniting *M. badius* with the remaining cowbirds has an additional consequence for our understanding of the evolution of INTER. *Molothrus badius* is a nest parasite but rears its own young [a behavior found in many other bird species (*2*)]. If this species is the sister taxon to the parasitic cowbirds as has been assumed on behavioral grounds, then nest parasitism may be the preliminary step in the transformation series from nest building to generalized brood parasitism. Conversely, if any of the other nest-building blackbirds is the true sister taxon of the brood-parasitic cowbirds, then brood parasitism presumably evolved independently of the nest parasitism exhibited by *M. badius*.

REFERENCES AND NOTES

1. H. Friedmann, *The Cowbirds: A Study in the Biology of Social Parasitism* (Thomas, Springfield, IL, 1929).
2. R. B. Payne, *Annu. Rev. Ecol. Syst.* **8**, 1 (1977).
3. S. I. Rothstein, *ibid.* **21**, 481 (1990).
4. Explicit phylogenies are lacking for all brood parasites except cowbirds (*1*). Hamilton and Orians (*5*) suggested that this phylogeny, constructed from geographic distribution, courtship display, song, and plumage coloration, was probably misleading given the limited systematic value of these characters.
5. W. J. Hamilton, III, and G. H. Orians, *Condor* **67**, 361 (1965).
6. J. Felsenstein, *Am. Nat.* **125**, 1 (1985); M. Ridley, *The Explanation of Organic Diversity: The Comparative Method and Adaptations for Mating* (Oxford Univ. Press, Oxford, 1983); D. R. Brooks and D. A. McLennan, *Phylogeny, Ecology, and Behavior* (Univ. of Chicago Press, Chicago, 1991).
7. N. B. Davies and M. de L. Brooke, *J. Anim. Ecol.* **58**, 225 (1989).
8. Characterization of cowbird species as specialized, intermediate, or generalized with respect to host selection is based on the number of species recorded as hosts (*19*). Although it is true that other aspects of the birds' biology, such as range size, may influence the absolute number of species parasitized, the relative ranking of species is unaffected.
9. R. K. Saiki *et al.*, *Science* **239**, 487 (1988); U. B. Gyllensten and H. A. Erlich, *Proc. Natl. Acad. Sci. U.S.A.* **85**, 7652 (1988). Oligonucleotide primers from T. D. Kocher *et al.* [*ibid.* **86**, 6196 (1989)] used in this study were: L14841 5′-AAAAAGCTTCCATCCAACATCTCAGCATGATGAAA-3′; and H15149 5′-AAACTGCAGCCCCTCAGAATGATATTTGTCCTCA-3′. Other primers used were: L15042 5′-ATCTGCATCTACCTACACATCGG-3′; L15243 5′-ACCCTAGTAGAATGAGCCTGAGG-3′; and H15767 5′-GATGAATGGGTGTTCTACTGGTTG-3′, where L and H refer to light and heavy strands respectively; numbers correspond to the location of the 3′ end of the primer in the human mtDNA sequence as reported by S. Anderson *et al.* [*Nature* **290**, 457 (1981)]. DNA was extracted from samples of pectoral muscle frozen initially in liquid nitrogen under field conditions and subsequently stored at −70°C.
10. F. Sanger, S. Nicklein, A. R. Coulson, *Proc. Natl. Acad. Sci. U.S.A.* **74**, 5463 (1977).
11. *Psarocolius decumanus, P. yuracares, Cacicus cela, C. holosericeus, Nesopsar nigerrimus, Gymnomystax mexicanus, Xanthocephalus xanthocephalus, Agelaius ruficapillus, Sturnella militaris, S. neglecta, Pseudoleistes guirahuro, Amblyramphus holosericeus, Curaeus curaeus, Gnorimopsar chopi, Macroagelaius subalaris, Dives dives, Quiscalus quiscula, Q. niger, Euphagus cyanocephalus, Dolichonyx oryzivorus, Passerina cyanea, Saltator coerulescens.*
12. Sequence data were analyzed by the exhaustive search option of PAUP [D. L. Swofford, *PAUP: Phylogenetic Analysis Using Parsimony Version 3.0L* (Illinois Natural History Survey, Urbana, IL, 1985)].
13. S. M. Lanyon, *Syst. Zool.* **34**, 397 (1985).
14. J. Felsenstein, *Evolution* **39**, 783 (1985).
15. F. C. Rohwer and S. Freeman, *Can. J. Zool.* **67**, 239 (1989).
16. W. H. Hudson, *Birds of La Plata* (J. M. Dent, New York, 1920), pp. 105–106.
17. R. M. Fraga, *Wilson Bull.* **91**, 151 (1979).
18. P. Desjardins and R. Morais, *J. Mol. Biol.* **212**, 599 (1990).
19. G. H. Orians, *Blackbirds of the Americas* (Univ. of Washington Press, Seattle, 1985).

20. Supported by NSF grant BSR-8614240 and by the Ellen Thorne Smith Fund. Laboratory work was conducted at the FMNH biosystematics laboratory by P. Austin and J. Briggs. S. Cardiff, D. Dittman, J. Fitzpatrick, D. Stotz, D. Willard, and the staff of the Louisiana State University Museum of Zoology assisted in obtaining the tissue samples. S. Goodman, J. Hall, P. Lowther, T. Peterson, T. Schulenberg, and D. Willard provided helpful comments on this manuscript.

22 July 1991; accepted 8 October 1991

Activation of T Cells by a Tyrosine Kinase Activation Domain in the Cytoplasmic Tail of CD3 ϵ

FRANÇOIS LETOURNEUR AND RICHARD D. KLAUSNER

The multichain T cell antigen receptor functions by interacting with and activating one or more nonreceptor tyrosine kinases. The cytoplasmic tail of the ζ chain can activate T cells independently of the rest of the receptor complex. The function of the remaining invariant CD3 chains remains unknown. A 22–amino acid region of the cytoplasmic tail of CD3 ϵ was also able to independently activate T cells. Stimulation of T cells by means of the cytoplasmic tails of either ζ or CD3 ϵ resulted in quantitatively distinct patterns of tyrosine phosphorylation, suggesting activation of different biochemical pathways.

THE ABILITY OF ANTIGEN RECEPTORS to transduce signals to multiple biochemical cascades is the central event of immune cell activation. For the T cell antigen receptor (TCR), one or more Tyr kinases likely have a proximal and essential participation in T cell activation (*1*). Exactly how the receptor couples to its activation pathways is not clear. Evidence that the receptor complex associates with the Fyn Tyr kinase suggests that Fyn may be one potential mediator of early biochemical events (*2*). The receptor is an eight-chain transmembrane complex composed of four dimers (*3*). The clonotypic chains (generally α and β) provide the ligand specificity (*4*). The invariant dimers, including CD3 ϵ-γ, CD3 ϵ-δ, and ζ-ζ (*3, 5, 6*), are probably essential for signal transduction, as demonstrated by mutational analysis of the cytoplasmic tail of ζ (*7*). This domain of ζ can mediate the signaling events associated with TCR-mediated activation when expressed in a chimeric transmembrane protein (*8–10*). Two observations, however, suggest that ζ alone does not account for all of the func-

Cell Biology and Metabolism Branch, National Institute of Child Health and Human Development, National Institutes of Health, Bethesda, MD 20892.

Fig. 1. (**A**) Schematic representation of chimeric Tac proteins with external (EX), and transmembrane (TM), and cytoplasmic (CY) ϵ domains. Plain lines correspond to conserved residues, and dotted lines show deleted sequences. Chimeras and mutants were constructed by polymerase chain reaction (*19*) and cloned into pCDL SRα (*20*) and sequenced. (**B**) Mutational analysis of the Tyr kinase activation domain of CD3 ϵ. Point mutations are denoted by the amino acid mutagenized, followed by the residue substituted and its position number (for example, LA180). The effect of each individual point mutation on function was assessed as described in Fig. 3 by transient transfection. IL-2 production similar to that obtained with the native Tac-ϵ chimera is denoted with a plus (+) symbol, and a minus (−) corresponds to no detectable signal. For mutations LA180 and SL182, the asterisk signifies an IL-2 secretion that is 88 and 69% of control, respectively, after maximal stimulation. Abbreviations for the amino acid residues are as follows: A, Ala; C, Cys; D, Asp; E, Glu; F, Phe; G, Gly; H, His; I, Ile; K, Lys; L, Leu; M, Met; N, Asn; P, Pro; Q, Gln; R, Arg; S, Ser; T, Thr; V, Val; W, Trp; and Y, Tyr.

Table 1. Flow cytofluorometry of stable and transient BW transfectants. The indicated cells were labeled with MAbs to Tac (33B3.1) (Amac, Westbrook, Maine), CD3 ϵ (2C11) (*17*), or Thy-1 (G7) (*18*) and then labeled with fluorescein-conjugated rabbit antibody to rat immunoglobulin (Cappel). Samples were analyzed with a FACScan (Becton Dickinson). Transient transfectants are denoted by the name of the transfected chimera.

Labeled cell	Linear fluorescence (mean)			Chimera (% positive)
	2C11	33B3.1	G7	
2B4	18.0	2.9	167.4	
BW	3.2	3.6	151.7	
Stable transfectants				
TTζ clone 4	2.8	230.1	220.1	100
TTζ clone 7	3.2	682.4	245.2	100
TTϵ clone 5	3.0	517.0	172.3	100
TTϵ clone 8	2.9	257.0	208.4	100
TTϵ clone 9	2.8	117.1	231.2	100
TTϵ.178 clone 2	3.3	186.2	182.0	100
TTϵ.178 clone 11	3.2	350.9	274.0	100
Transient transfectants				
BW (untransfected)		4.4		
TTϵ		70.2		54.9
Tζϵ		63.6		47.8
TTϵ NL185		73.3		50.9
TTϵ GL183		75.4		59.1
TTϵ YL181		88.4		53.5
TTϵ YF181		68.9		50.2
TTϵ.Del		77.9		50.4
TT66/178		88.8		58.0
TT66/168		83.2		54.5

tional capacity of the TCR complex. First, in the absence of any ζ protein, the small number of incomplete TCR complexes that are transported to the cell surface can signal when externally cross-linked (*11*). Second, extensive cytoplasmic tail deletions of ζ could reconstitute surface expression of functional TCR complexes in a ζ-deficient thymoma, even when the analogous ζ chimeric constructs were not active (*12*). We therefore used the chimeric subunit approach to assess the signaling and activation capacity of the cytoplasmic tail of the CD3 ϵ chain.

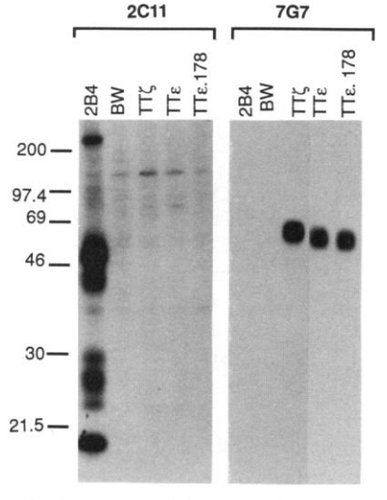

Fig. 2. Immunoprecipitations of surface-iodinated cells. Stable transfectants were obtained by electroporation of an αβ-negative variant of BW 5147 (*13*) referred to as BW. Cells (2B4, BW, TTζ clone 4, TTϵ clone 8, and TTϵ.178 clone 11) (4×10^7) were labeled with 1 mCi of ^{125}I by lactoperoxidase-catalyzed iodination (*6*) and solubilized at 4°C in 0.5% Triton X-100 lysis buffer. Lysates were incubated with protein A–Sepharose (Gibco-BRL) bound either with MAb to CD3ϵ (2C11) (*17*) or MAb to Tac (7G7) (*21*). Immunoprecipitates were analyzed on 13% SDS–polyacrylamide gels. The relative positions of the molecular size standards are indicated at left in kilodaltons.

We constructed chimeric proteins by replacing the cytoplasmic tail of the human interleukin-2 (IL-2) receptor α chain (the Tac antigen) with the cytoplasmic tail of murine ζ or CD3 ϵ. These chimeras were stably transfected into BW 5147 cells that do not synthesize α, β, δ, and ζ or detectable TCR components on the cell surface (*13*). Cells stably expressing Tac-ζ (TTζ), Tac-ϵ (TTϵ), or Tac-ϵ with a stop codon at Arg^{178} (TTϵ.178) (Fig. 1) were cloned and examined for surface expression of the introduced proteins by flow cytofluorometry (Table 1). In addition, the cells were iodinated, and the proteins were immunoprecipitated with monoclonal antibodies (MAbs) to the external domains of either CD3 ϵ (MAb 2C11) or Tac (MAb 7G7) (Fig. 2). MAb 2C11 did not label or immunoprecipitate any specific proteins from the transfectants or the parental BW cells. However, the TCR-positive hybridoma 2B4 did react with MAb 2C11. In contrast, MAb 7G7 precipitated a single band of the predicted size for each of the chimeric proteins. No coprecipitated CD3 ϵ or γ subunits were seen, even after overexposure of the autoradiograms. Flow cytofluorometry revealed two- to threefold variations in expression by individual clones, so multiple clones for each construct were evaluated. In addition, transient transfections were done with other constructs (Fig. 1), and flow cytofluorometry revealed comparable cell surface expression (Table 1).

The stably transfected clones were tested for IL-2 secretion in response to cross-linking with a MAb to Tac (33B3.1) (Fig. 3A). BW cells alone or transfected with TTϵ.178 produced no IL-2 in response to this treatment. Clones of each chimeric construct, despite three- to fourfold differences in surface expression of the chimeric protein, had equivalent IL-2 production when stimulated, demonstrating that the surface receptor levels, over this range, are not limiting for responsiveness. Tac-ζ was most effective at IL-2 production, but at sufficient doses of MAb 33B3.1 Tac-ϵ produced as much IL-2 as Tac-ζ. In contrast, the Tac-ϵ deletion mutant gave no detectable IL-2 at any dose of MAb 33B3.1 tested. All clones produced relatively similar concentrations of IL-2 in response to the pharmacologic activators phorbol 12-myristate 13-acetate and calcium ionophore.

We tested whether further mutational analysis could isolate the region of the ϵ tail critical for cell activation. A variety of mu-

tants were constructed (Fig. 1A) and tested for IL-2 secretion after cross-linking of transiently transfected BW cells (Fig. 3, B and C). The cytoplasmic tail of ε contains 55 amino acids. Removal of the terminal 12– or 22–amino acid residues (TTε.178 and TTε.168) abrogates IL-2 production. In contrast, an internal deletion of 12 amino acids (TTε.Del) had no effect on IL-2 production. To test whether the terminal sequences of ε can confer activation capacity on an unrelated and inactive cytoplasmic tail sequence, we fused the COOH-terminal 12– or 22–amino acid residues to the construct called TT66 (and produced TT66/178 and TT66/168, respectively). TT66 contains the membrane-proximal 14–amino acid residues of the cytoplasmic tail of ζ, which has no ability to signal (*10*). TT66/178 results in no IL-2 production, whereas TT66/168 results in high IL-2 production. Thus, the terminal 22–amino acid residues of ε contain independent information for signaling. Although structures in the COOH-terminal half of this region are essential for activity, the terminal amino 12–acid residues alone are insufficient for coupling.

In order to identify residues that are critical for function, we mutated each residue of the terminal 22 amino acids of ε. The mutated Tac-ε chimeras were then expressed and assayed for IL-2 production. Effects of mutation on residues Tyr^{181}, Gly^{183}, and Asn^{185} are shown Fig. 3. Complete analysis of each mutation is compiled in Fig. 1B. Two critical regions can be defined. The first region includes residues Tyr^{170}, Glu^{171}, Pro^{172}, and Ile^{173}. The second region includes residues Asp^{179} and Tyr^{181}. For both groups, any tested mutation resulted in complete inactivation of the Tac-ε chimera. Residues Leu^{180} and Ser^{182} showed partial IL-2 production when changed Ala and Leu, respectively. All other residues (Fig. 1B) could be changed with no effect on IL-2 production, although deletion of two residues between the two critical regions destroyed function.

We examined whether Tac-ζ or Tac-ε, both of which contain cytoplasmic Tyr, were phosphorylated on Tyr when cross-linked by MAb to Tac (anti-Tac). This was determined by immunoprecipitation of the chimeric proteins from control and stimulated cells, followed by immunoblotting with 4G10, an antibody to phosphotyrosine. Whereas Tac-ζ was phosphorylated after activation, little if any signal could be detected for Tac-ε (Fig. 4A), despite equivalent amounts of chimeric proteins on the gel. Phosphopeptide analysis of activated, ^{32}P-labeled cells confirmed the absence of Tyr phosphorylation of Tac-ε chimera and the presence of high Ser phosphorylation.

To examine Tyr kinase activity after chimera cross-linking, we immunoprecipitated with MAb 4G10 (to phosphotyrosine) and then immunoblotted with 4G10. Cross-linking of both chimeras led to the Tyr phosphorylation of multiple intracellular substrates (Fig. 4B). Maximum doses of anti-Tac were used, which resulted in equiv-

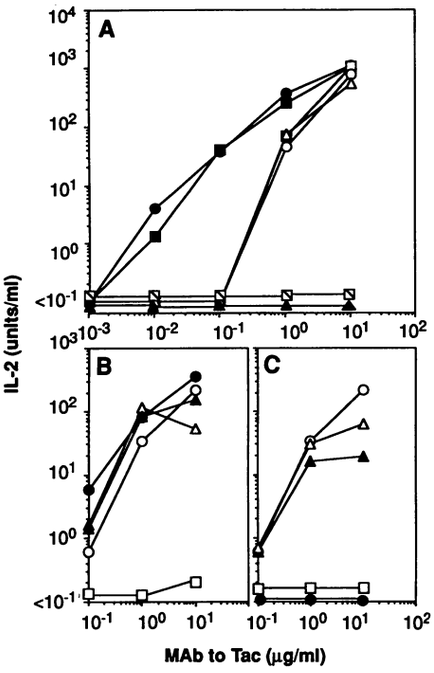

Fig. 3. (**A**) IL-2 production of stable transfectants in response to cross-linking with antibody to Tac. Transfectants (10^5 cells) were cultured in duplicate in 96-well plates coated with the indicated concentrations of 33B3.1 (*10*). Supernatants were harvested after 24 hours of culture, and IL-2 content was determined (*22*). Closed circles, TTζ clone 4; closed squares, TTζ clone 7; open squares, TTε clone 5; open circles, TTε clone 8; open triangles, TTε clone 9; closed triangles, TTε.178 clone 2; and open squares with diagonal line, TTε.178 clone 11. (**B** and **C**) IL-2 production of BW cells transiently transfected with Tac-ε mutants. BW cells (10^7) were transfected with the DEAE-dextran method (*23*). After 24 hours of culture, cells were stimulated with MAb to Tac as described above. Results were reproduced at least twice for each mutant without significant variations. We biochemically examined the proteins made by the transfectants to ensure the correct size. Symbols in (B) denote the following: open circles, TTε; closed circles, Tζε, Tac with ζ transfectant and an ε cytoplasmic tail; open triangles, NL185; closed triangles, GL183; and open squares, YL181. Symbols in (C) denote the following: open circles, TTε; closed circles, YF181; open triangles, TTεDel; closed triangles, TT66/168; and open squares, TT66/178.

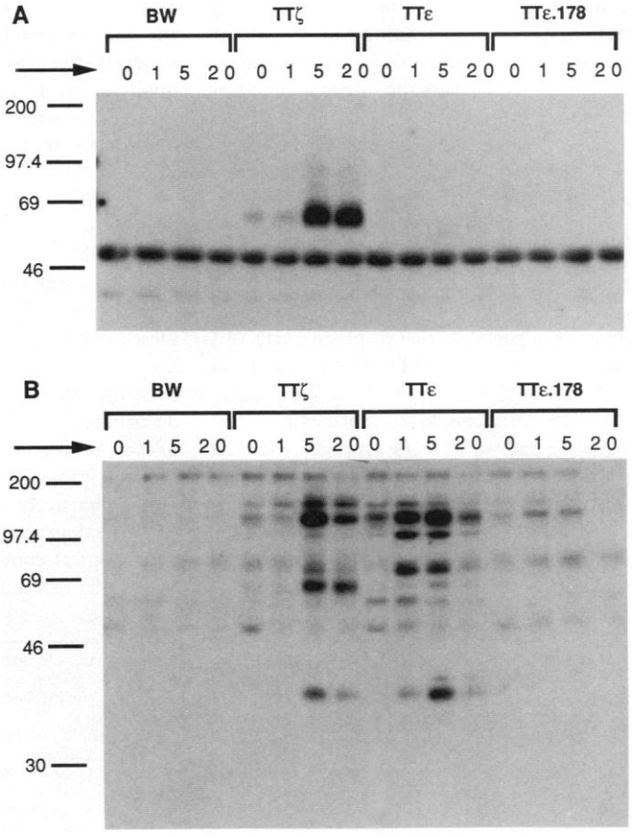

Fig. 4. (**A**) Tac-ζ chimera, in contrast to Tac-ε, is phosphorylated on Tyr after anti-Tac cross-linking by antibody to Tac. (**B**) Stimulation of both Tac-ζ and Tac-ε chimeras results in Tyr kinase substrate phosphorylation. Cells (BW, TTζ clone 4, TTε clone 8 and TTε.178 clone 11) (2×10^7 per well) were incubated for 30 min at 37°C with 5 μg of biotinylated MAb to Tac (IOT 14) (Amac). After centrifugation, cells were stimulated in 0.6 ml of serum-free medium containing 12 μg of avidin (Sigma). After the incubation times indicated at the top of each lane, cells were lysed in modified RIPA buffer (1% NP-40, 0.25% sodium deoxycholate, 150 mM NaCl, and 50 mM tris, pH 7.5) containing phosphatase inhibitors (2 mM EDTA and 1 mM vanadate). Chimeras were immunoprecipitated with MAb 7G7 (A) or the MAb to phosphotyrosine 4G10 (Upstate Biotechnology, Lake Placid, New York) (B), as described in Fig. 2. Beads were washed three times in modified RIPA buffer, followed by one wash in TN buffer (50 mM tris, pH 7.5, and 150 mM NaCl). Immunoprecipitates were analyzed on 10% SDS–polyacrylamide gels, transferred to nitrocellulose, and immunoblotted (*14*) with MAb 4G10, followed by ^{125}I-labeled protein A. Molecular size standards are indicated at left in kilodaltons.

alent amounts of IL-2 production from the two chimeras. For both activated constructs, multiple substrates are apparent; phosphorylation activity rose rapidly over 5 min and then fell by 20 min. A reproducible difference in the substrate patterns for the two constructs was observed. Whereas several of the substrates were shared (for example, 120 and 36 kD), others are differentially phosphorylated. Tac-ζ resulted in the more prominent appearance of substrates at 140 and 65 kD (which represented the chimeric protein), whereas Tac-ε resulted in the prominent appearance of substrates at 100, 72 to 75, 67, and 38 kD. The 100-kD Tac-ε substrate comigrates with a prominent substrate seen in BW-fused T cell hybridomas and in human peripheral blood lymphocytes after stimulation of the intact TCR complex (*14, 15*). These differences suggest that the biochemical consequences of signaling through the ζ and ε tails are distinct. Whether this reflects the activation of different Tyr kinases must be addressed; these results raise the possibility that these two signaling-competent cytoplasmic tails of the TCR may provide distinct information to the cell.

Our data show that at least two subunits of the eight-chain TCR complex are independently capable of signal transduction, leading to both Tyr kinase activation and the production of IL-2. The ability of CD3 ε, in addition to ζ, to signal resolves the dilemma raised by the findings that the cytoplasmic tail of ζ alone can mimic TCR-mediated activation (*8–10*), yet partial TCR complexes lacking any ζ chain can activate hybridoma cells to produce IL-2 (*11*). The presence of two proteins in a single receptor complex independently able to transduce signals raises several questions about the functioning of the intact receptor. Are the cytoplasmic tails of ζ and CD3 ε redundant? Do they cooperate in the activation of the same signaling pathways? Do they couple to similar but distinct signaling pathways? Some support for the last possibility is suggested by the difference in substrate phosphorylation patterns produced by the Tac-ζ and Tac-ε chimeras. Thus, the multichain TCR complex may not generate signals through a single subunit. The 22–amino acid functional motif of CD3 ε described here can be aligned to a consensus sequence present in the COOH-terminal domains of subunits of various receptors (*16*). Whether this represents an identical coupling motif or variations on a general theme, perhaps for preferential coupling to different Src family kinases, can now be addressed.

REFERENCES AND NOTES

1. R. D. Klausner and L. E. Samelson, *Cell* **64**, 875 (1991).
2. L. E. Samelson, A. F. Philipps, E. T. Luong, R. D. Klausner, *Proc. Natl. Acad. Sci. U.S.A.* **87**, 4358 (1990).
3. N. Manolios, F. Letourneur, J. S. Bonifacino, R. D. Klausner, *EMBO J.* **10**, 1643 (1991).
4. R. H. Schwartz, *Annu. Rev. Immunol.* **3**, 237 (1985).
5. F. Konig, W. L. Maloy, J. E. Coligan, *Eur. J. Immunol.* **20**, 299 (1990).
6. L. E. Samelson, J. B. Harford, R. D. Klausner, *Cell* **43**, 223 (1985).
7. S. J. Frank *et al.*, *Science* **249**, 174 (1990).
8. B. A. Irving and A. Weiss, *Cell* **64**, 891 (1991).
9. C. Romeo and B. Seed, *ibid.*, p. 1037.
10. F. Letourneur and R. D. Klausner, *Proc. Natl. Acad. Sci. U.S.A.* **88**, 8905 (1991).
11. J. J. Sussman *et al.*, *Cell* **52**, 85 (1985).
12. F. Letourneur and B. Malissen, in preparation.
13. J. White *et al.*, *J. Immunol.* **143**, 1822 (1989).
14. E. Hsi *et al.*, *J. Biol. Chem.* **264**, 10836 (1989).
15. C. H. June, M. C. Fletcher, J. A. Ledbetter, L. E. Samelson, *J. Immunol.* **144**, 1591 (1990).
16. M. Reith, *Nature* **338**, 383 (1983).
17. O. Leo, M. Foo, D. H. Sachs, L. E. Samelson, J. A. Bluestone, *Proc. Natl. Acad. Sci. U.S.A.* **84**, 1374 (1987).
18. K. C. Gunter, T. R. Malek, E. M. Shevach, *J. Exp. Med.* **159**, 716 (1984).
19. R. Higuchi, B. Krummel, R. Saiki, *Nucleic Acids Res.* **16**, 7351 (1988).
20. Y. Takebe *et al.*, *Mol. Cell. Biol.* **8**, 466 (1988).
21. L. A. Rubin, C. C. Kurman, W. E. Biddison, N. D. Goldman, D. L. Nelson, *Hybridoma* **4**, 91 (1985).
22. J. D. Ashwell, R. E. Cunningham, P. D. Noguchi, D. Hermandez, *J. Exp. Med.* **165**, 173 (1987).
23. R. F. Seldin, *Current Protocols in Molecular Biology* (Greene and Wiley-Interscience, New York, 1990), vol. 1, pp. 921–926.

24. We thank L. E. Samelson and J. Bonifacino for critical review of the manuscript.

2 August 1991; accepted 15 October 1991

Torsional Rigidity of Positively and Negatively Supercoiled DNA

PAUL R. SELVIN,* DAVID N. COOK, NING G. PON, WILLIAM R. BAUER, MELVIN P. KLEIN, JOHN E. HEARST

Time-correlated single-photon counting of intercalated ethidium bromide was used to measure the torsion constants of positively supercoiled, relaxed, and negatively supercoiled pBR322 DNA, which range in superhelix density from +0.042 to −0.123. DNA behaves as coupled, nonlinear torsional pendulums under superhelical stress, and the anharmonic term in the Hamiltonian is approximately 15 percent for root-mean-square fluctuations in twist at room temperature. At the level of secondary structure, positively supercoiled DNA is significantly more flexible than negatively supercoiled DNA. These results exclude certain models that account for differential binding affinity of proteins to positively and negatively supercoiled DNA.

THE MOTIVATION FOR STUDYING the torsional rigidity of supercoiled DNA is threefold. First, such study provides a stringent test of current theoretical models of DNA that assume that the twisting (and bending) internal forces are harmonic and isotropic (*1, 2*). Second, the twisting rigidity of DNA is an important determinant of the energetics of formation of complicated nucleoprotein structures (*3*). Third, although the torsion constant has been extensively studied for linear DNA (*4–8*), its dependence on superhelicity under physiological conditions has not been systematically measured.

P. R. Selvin, Department of Physics, University of California, Berkeley, and Laboratory of Chemical Biodynamics, Lawrence Berkeley Laboratory, Berkeley, CA 94720.
D. N. Cook, N. G. Pon, J. E. Hearst, Department of Chemistry, University of California, Berkeley, and Laboratory of Chemical Biodynamics, Lawrence Berkeley Laboratory, Berkeley, CA 94720.
W. R. Bauer, Department of Microbiology, School of Medicine, State University of New York, Stony Brook, NY 11794.
M. P. Klein, Laboratory of Chemical Biodynamics, Lawrence Berkeley Laboratory, Berkeley, CA 94720.

*To whom correspondence should be addressed; present address: Laboratory of Chemical Biodynamics.

We obtained torsion constants by fitting the fluorescence anisotropy decay of ethidium bromide intercalated in various supercoiled topoisomers of pBR322 to the theory of Barkley and Zimm with the use of a Marquardt-based algorithm (*2, 9*). The anisotropy decay arises from the reorientation of excited-state ethidium bromide due to the twisting (and bending) of the DNA helix, and it was detected by time-correlated single-photon counting. The Barkley-Zimm theory, which models DNA as a uniform elastic rod that bends and twists in a viscous medium, is a harmonic approximation. The fitted value of the torsion constant depends weakly on the bending rigidity chosen, which we assume is constant and independent of superhelicity. Because of the weak dependence on bending and the fact that DNA is not severely bent in a plectonemic superhelix (*10*), this assumption is justified.

We chose a bending constant that yields a persistence length of 525 Å. We also analyzed the data with the exclusion of the effect of bending (infinite bending constant), which yields a lower limit to the torsion constant. In this limit, the Allison-Schurr and Barkley-Zimm models of DNA dynam-